

Preliminary Studies on Protein-Aided Nanoparticle Interactions

by

Luqmanal Hakim Sirajudeen

A Thesis Presented in Partial Fulfillment  
of the Requirements for the Degree  
Master of Science

Approved September 2019 by the  
Graduate Supervisory Committee:

Brent L. Nannenga, Chair  
Abhinav Acharya  
Jeremy Mills

ARIZONA STATE UNIVERSITY

December 2019

## ABSTRACT

This work aims to characterize protein-nanoparticle interactions through the application of experimental techniques to aid in controlled nanoparticle production for various applications from manufacturing through medical to defense. It includes multiple steps to obtain purified and characterized protein and then the production of nanoparticles using the protein. This application of protein requires extremely pure homogenous solution of the protein that was achieved using numerous protein separation techniques which were experimented with. Crystallization conditions, protein separation methods and protein characterization methods were all investigated along with the protein-nanoparticle interaction studies. The main protein of study here is GroEL and the inorganic nanoparticle used is platinum. Some studies on MBP producing gold nanoparticles from an ionic gold precursor were also conducted to get a better perspective on nanoparticle formation. Protein purification methods, crystallization conditions, Car-9 tag testing and protein characterization methods were all investigated along with the focus of this work. It was concluded that more Car9 studies need to be carried out before being used as in the form of a loop in the protein. The nanoparticle experiments were successful and platinum nanoparticles were successfully synthesized using GroEL. The direction of further research in protein-nanoparticle studies are outlined towards the end of the thesis.

## ACKNOWLEDGEMENTS

As I complete my Masters degree, I look back and reflect on my college career up to this point and remember all the individuals who have the person I am today. I would like to thank every single person that has influenced my life in a positive way and the ones who have stuck by me to achieve the completion of not one but two degrees. I shall now attempt to give credit to some of the most important people who have helped me achieve this milestone in my life.

I shall begin with my advisor Dr. Brent Nannenga who welcomed me into his lab as a masters student to work on projects that would go on to become the core of my masters thesis. Dr. Nannenga is a hard-working and intellectual individual whose passion for his line of work has been a great source of inspiration as well as a driving force in my years of research under him. He has helped me through many difficulties and has always been an exceptional source of guidance. It was a great honor to work under Dr. Nannenga and to have achieved my goals under his mentorship. I would also like to thank Amar and Guan hong, who are members of the Nannenga Lab, for their extensive help and support in my work and being my support since Day 1.

Most importantly, I am extremely thankful for my parents Mohamed and Mumtaz for being a never-ending source of support, care and love through my hard as well as easy days. My parents will always take a huge chunk of the credit for whatever I have achieved till today and whatever I will achieve in the future as they have stood by me no matter the

situation. I would also like to thank my sister Sumayya for being a source of support in my life. Last but not least, I would like to thank my close friends who have always supported and motivated me and shown me nothing but love.

I will be eternally indebted to you all.

## TABLE OF CONTENTS

	Page
LIST OF FIGURES .....	vi
CHAPTER	
1 INTRODUCTION .....	1
1.1 Interaction of Proteins and Inorganic Materials.....	1
1.1.1 Nature and History of Biomineralization.....	2
1.1.2 Modern Day Applications.....	3
1.2 Metal Nanoparticles .....	5
1.3 Experimental Overview .....	6
2 INTERACTION OF GroEL WITH PLATINUM .....	8
2.1 Experimental Materials and Methods .....	9
2.1.1 GroEL Expression.....	9
2.1.2 GroEL Purification.....	10
2.1.2.1 Lysis and Rudimentary Purification .....	11
2.1.2.2 Advanced Purification .....	12
2.1.3 GroEL Characterization .....	15
2.1.4 Assembly and Characterization of Platinum Nanoparticles .....	16
2.1.5 Crystallization of GroEL.....	16

2.2	Results and Discussion .....	17
CHAPTER		Page
3	INTERACTION OF MBP WITH GOLD.....	28
3.1	Experimental Materials and Methods .....	29
3.1.1	MBP Expression and Purification.....	29
3.1.2	Assembly of Gold Nanoparticles .....	29
3.2	Results and Discussion .....	30
4	Car9 TAG STUDIES .....	33
4.1	Introduction to the Car9 Tag.....	33
4.2	Materials and Methods.....	34
4.3	Results and Discussion .....	35
5	CONCLUSIONS AND FUTURE WORK .....	42
5.1	Inorganic Nanoparticle Synthesis Using Proteins and Peptides .....	42
5.2	Car9 Tag.....	43
REFERENCES .....		44

## LIST OF FIGURES

Figure	Page
1. Load and Wash Steps of IE Chromatogram of GroEL where the Lack Line Shows the % Of Elution Buffer, Blue Line Shows the Absorbance at 280 nm which Indicates Protein Presence and the Red Line Shows the Conductivity .....	17
2. The Elution Part of the IE Chromatogram for GroEL .....	18
3. SDS-PAGE Gel of the IEC Step in GroEL Purification Shown from the Above Chromatogram Pictures Along with the Collected SEC Fractions After the IEC, where FT Refers to Flow Through, W Refers to Wash .....	18
4. Chromatogram of The SEC Step Performed After Heat Purification Step Applied to GroEL Lysate.....	19
5. SDS-PAGE Gel of the Above SEC Step for GroEL Purification Using Heat Shock Method .....	19
6. A Photograph of GroEL Crystals Formed when GroEL Concentration was at 40mg/ml (1:1 On Pedestal) and Reservoir Solution Consisted Of 0.1M Sodium Citrate at pH 5.3, 11% PEG 6000 .....	20
7. A Photograph of GroEL Crystals that Formed when GroEL Concentration was at 40mg/ml (1:1 on Pedestal) and Reservoir Solution Consisted of 0.1M Sodium Citrate at pH 5.4, 9% PEG 6000 .....	21

Figure	Page
8. A Photograph of GroEL Crystals that Formed when GroEL Concentration was 54 mg/ml (1:1 – Protein:Reagent on Pedestal) and Reservoir Solution Consisted of 0.3% PEG 8000, 1.72M Ammonium Sulfate, 0.004M Calcium Chloride and 0.1M Tris-HCl at pH 8.0 .....	21
9. Eppendorf Tubes Holding Metallic Platinum Reduced from Ions by NaBH <sub>4</sub> in the Absence of Protein (Left) and Platinum Nanoparticles in the Presence of GroEL (Right) .....	23
10. GroEL in the Presence of Platinum Ions (K <sub>2</sub> PtCl <sub>4</sub> ): Left – Immediately After Addition, Right – After Storage for a Month.....	23
11. Eppendorf Tubes Showing the Comparison of Platinum Nanoparticle Formation Using GroEL (Two Tubes on the Left) Versus Bulk Platinum Formation in the Absence of GroEL .....	24
12. Low Contrast Photograph of Platinum Nanoparticles Versus Bulk Platinum.....	24
13. 3D Reconstruction of GroEL (Top View) Showing Two Regions of Higher Density in the Center Cavity .....	25
14. Side View of 3D Reconstruction of GroEL Showing the Higher Density Regions in the Center when Superimposed with the 3D Structure of Only GroEL .....	26
15. CryoEM Pictures After Data Refining Showing a Distinct Region of Hypothesized Nanoparticle Formation Inside the GroEL Cavity.....	26
16. Data of the Wavelength Scan at t=18 Hours of Different Peptides Including a Control Peptide .....	31

Figure	Page
17. SDS-PAGE Gel Showing Elution Fractions of sfGFP:: <i>Car9</i> -5aa Flowing Through a Silica Bed in a Gravity Column After Being Incubated in the Silica Resin for 16 Hours at 4°C.....	35
18. SDS PAGE Gel Showing the Elution Volumes for sfGFP:: <i>Car9</i> when Flowing the Lysate Through the Silica Bed in a Gravity Column After Incubation for 16 Hours at 4°C .....	36
19. A Photograph of the SDS-PAGE Gel of the Fractions Collected by Flowing Wildtype GroEL Through a Silica Resin Bed and Eluted Using 1M L-Lysine ....	37
20. A Photograph of the SDS-PAGE Gel Analysis of the Fractions Collected when GroEL Containing the <i>Car9</i> Tag in a Loop was Flowed Through Silica Resin and Eluted with 1M L-Lysine.....	38
21. ONPG Test Results of the $\beta$ -Galactosidase Samples in the <i>Car9</i> Testing: 1 - Load, 2 - Flow Through, 3 - Wash, 4 - Elution using 1M L-Lysine.....	40
22. Eppendorf Tube After Incubation with ONPG Showing the Silica Resin Region Displaying Very Little to No Yellow Color but the Supernatant Showing a Bright Yellow Color.....	41

## Chapter 1

### INTRODUCTION

Proteins are one of the most fundamental building blocks of life. They perform a wide range of functions from something as simple as providing structural support all the way to catalyzing complex reactions. Since proteins are essentially the basis of life, they have been studied extensively and are being used to find cures to diseases at the forefront of the medical field and are being used to manufacture complex inorganic and organic structures in the industrial level. Proteins come in a large number of sizes, shapes and functions and can be easily modified through genetic mutations which makes it a very versatile platform to work with.

#### 1.1 Interactions of Proteins and Inorganic Materials

Proteins have been studied to interact with variety of inorganic materials both in nature as well as in an artificial setup. More recent discoveries such as interaction of proteins with negatively charged surfaces have excited researchers as more proof of interaction with inorganic material has been discovered. This means that the uses of proteins can be broadened towards manufacturing or medical applications such as drug delivery, biomaterial and particle synthesis. The interaction of proteins with inorganic materials has been traced back to the amino acids that make up the protein as well as the

structure of the protein. In some cases, mineral ions are essential in order to transport other materials or for other essential processes. A popular example of this is the bioluminescent jellyfish *Aequoria Victoria*. This jellyfish contains two major bioluminescent proteins which are Aequorin and Green Fluorescent Protein (GFP). Calcium ions bind to aequorin which causes the release of visible light in the blue wavelength range. This blue light in turn is absorbed by the GFP which excites the fluorophore and releases visible light in the green wavelength range. Proteins interact with inorganic materials in a multitude of ways but for nanoparticle synthesis, the focus is on the topic of biomineralization.

#### 1.1.1. Nature and History of Biomineralization

Biomineralization is described as a process that living forms utilize to assist in the precipitation of minerals. Many instances of biomineralization has been known for a while but a lot of research and existing knowledge of biomineralization has been largely in macrostructures such as teeth and bones in humans and shells in some sea life forms.<sup>1</sup> The fact that we are able to find fossils is proof that nature has been biomineralizing for an extremely long time. In fact, the ability to biomineralize and form complex but integral structural components from minerals marks the beginning of the Cambrian era, which was around 541 million years ago, marked significant changes to life on earth. This allowed organisms to get more complex due to more structural support provided by the minerals. However, the oldest recorded proof of mineralization which corresponds to the oldest recorded proof of life on earth was from around 3.7 billion years old when biological

mineralized assemblies were found in fossilized hydrothermal vent precipitates.<sup>2</sup> With the evolution of biomineralization, organisms were able to evolve into more complex creatures which in turn helped in the evolution of more complex biomineralization techniques and processes.

Biomineralization can be categorized into two broad categories which are Biologically Induced Mineralization (BIM) and Biologically Controlled Mineralization (BCM). In BCM, the mineralization is directly controlled by a biological entity and is responsible for creation of very accurate and controlled structures such as bones and teeth in land and sea animals including humans. BCM also is very precise in controlling the crystalline structure of the final mineral structure which can be very helpful when exploited for any required purposes. On the other hand, BIM occurs when a living form creates a microenvironment that supports or promotes mineralization and does not provide much control over the mineralization process and which translates to less control over the characteristics of the final mineral product.<sup>1</sup>

#### 1.1.2. Modern Day Applications

Biomineralization is one of the oldest known cellular processes and it has evolved and been integrated into much more dynamic and complex processes in living beings. Extensive research has been carried out on various types of biomineralization and interaction of biology with inorganic materials. But recent evolution of nanoparticles and

nanotechnology has seen the emergence and development of nanobiotechnology. Some of the latest research in this field includes nanoscale protein-inorganic particle delivery machines and nanocrystal formations. There are some fascinating new studies that describe mineralization carried out by proteins and it is promising to help in the creation of advanced technology in the near future. The reason for this being so promising is that we lack the technology to fine-tune materials in the nanoscale and proteins (especially enzymes) can act as small molecular level machines and their high specificity for substrates along with their complex but extremely consistent structure provides the perfect platform for modified proteins to carry out biomineralization. Research in this direction has shown that proteins have the potential to create highly complex nanoscale structures at very high rates with extreme precision while also being efficient. *Plectonema boryanum*, a cyanobacteria, was used to produce gold nanoparticles from gold(I)-thiosulfate and gold(III)-chloride.<sup>3</sup> This study concluded that when *Plectonema boryanum* interacted with gold(I)-thiosulfate promoted the production of cubic (100) gold nanoparticles in membrane vesicles whereas when it interacted with gold(III)-chloride, production of octahedral (111) gold platelets in solutions and gold nanoparticles within the cells of the cyanobacteria.<sup>3</sup> In another study, gold nanoparticles were used to enhance the effectiveness of radiotherapy in mice with artificially induced tumor and concluded that the one-year survival was at 86% when the combination of gold nanoparticles and radiotherapy was used compared to only 20% when only radiotherapy was used.<sup>4</sup> The authors suggest that surface functionalization of the gold nanoparticles using antibodies that recognize tumors could be studied which would potentially increase the localized concentration of gold nanoparticles. But they do not

mention the shape or surface characteristics of the gold nanoparticles. The therapeutic application of gold nanoparticle is mainly because of its high resistance to oxidation and plasmon resonance. Plasmon resonance effect occurs when metallic nanoparticles interact with electromagnetic radiation of wavelengths much larger than the nanoparticle itself by absorbing and scattering the radiation. This leads to heating up of the nanoparticles due to the absorbed energy which results in a localized increase in temperature. This aspect is what allows metal nanoparticles to be of great importance in radiotherapy. The plasmonic resonance properties is dictated by the shape, size and surface features of the metal nanoparticle.<sup>5</sup> This is one of the many instances where precise control of the shape, size and surface features of nanoparticles that proteins could offer would greatly positively influence various industries such as manufacturing industries and therapeutic industries.

## 1.2 Metal Nanoparticles

Particles that lie in the size range from 1 nm to 100 nm are classified as nanoparticles. They can be further classified by shape as 0D, 1D, 2D or 3D or by materials such as metal or polymer nanoparticles. The reason for such high levels of interest in nanoparticles in modern days is due the unconventional reaction and interaction of nanoparticles with external stimuli or environments when compared to larger microscopic or macroscopic particles. This enables the application of nanoparticles in fields and applications where particles of other sizes would not be as effective. Some examples of this kind of application are in the medical field as drug delivery machines, colorimetric

assays, chemical and biological sensing, gas sensing, CO<sub>2</sub> sensors and a multitude of other applications.

Metal nanoparticles are very versatile in use especially in the medical field and one of the reasons for its popularity and versatility is the fact that it has special optoelectrical effects due to surface plasmon resonance.<sup>6</sup> Optoelectrical effects are the effects that are created when light in a system interacts with electronic effects in the system. Surface plasmon resonance is the resonant oscillation of electrons due to interaction with light.<sup>7</sup> This can be used to transfer energy efficiently in a very specific matter to or from a very localized area for therapeutic or other purposes.

### 1.3 Experimental Overview

This thesis work is broken down in chapters by the overall project theme. The study of interaction of protein with metal ions to produce protein nanoparticles is explored in Chapters 2 and 3. Chapter 2 focuses on the synthesis of platinum nanoparticles using GroEL while Chapter 3 involves in the study of the ability of MBP to produce gold nanoparticles. Chapter 4 explores the study of a novel amino acid tag that was developed to expedite the purification of proteins making use of specific interactions of peptides with inorganic materials. Protein purification steps in all the experiments were performed using common protein purification methods, the information for which are readily available from multiple sources. The final Chapter 5 is the culmination of documentation in this thesis

work which contains the conclusions of this work and some ideas for future work in protein-nanoparticle interaction and Car9 tag studies.

## Chapter 2

### INTERACTION OF GroEL WITH PLATINUM

GroEL is a chaperonin protein which belongs to the heat shock protein (Hsp60 class) and is made up of 14 subunits. Chaperonin proteins are those that are large multi-subunit assemblies which are essential for ATP-dependent polypeptide chain folding within the cell. Heat shock proteins are proteins that are over-expressed when the cell is exposed to a heat shock. GroEL is a ~800 kDa protein made of two large rings of 7 subunits each arranged in a 7-fold rotational symmetry with each subunit having a molecular mass of 57 kDa containing 547 amino acids. Structurally, it is a thick-walled cylinder that has a cavity in the center which provides favorable conditions for protein folding. GroEL has been isolated and expressed in the pET expression system that can be expressed using *E. coli* bacterial cells. A study conducted in 2012 concluded that GroEL facilitated the formation of platinum nanoparticles inside the cavity at the core.<sup>15</sup> The aim of this study is to verify the claims of the previous study and understand the mechanism of formation of platinum nanoparticles with the goal of being able to manipulate nanoparticle formation and create a simpler peptide that could form the platinum nanoparticle without the need for the entire GroEL structure which will make the nanoparticle formation more efficient.

## 2.1 Experimental Materials and Methods

### 2.1.1 GroEL Expression

Wild-type GroEL was expressed in *E. coli* cells using a *tac* promoter in a pET system. *tac* is a combination of *trp* and *lac* promoters. This offers a strong gene expression control as well as easy and efficient expression of the gene of interest using Isopropyl-beta-D-thiogalactoside (IPTG) that activates the *lac* operon by binding to the *lac* repressor. The system also uses T7 RNA polymerase in the pET system to selectively and efficiently overexpress the target gene of interest. T7 RNA polymerase is very active and is said to lead to a yield of induced cells consisting of the target protein accounting for up to 50% of the total cell content.<sup>9</sup> A GroEL stock was stored in -80° in around 20% glycerol from which all the cultures of GroEL are made from. A small amount of the stock is added to 5mL of Luria-Bertani (LB) broth (Miller). This has been the preferred medium for the growth of common bacterial strains since the 1950's.<sup>10</sup> The LB used here contains 10g/L tryptone, 10g/L NaCl and 5g/L yeast extract all of which are essential for the growth and multiplication of this strain of *E. coli* along with the appropriate antibiotic (which is Carbenicillin for the plasmid used here) at a concentration of 50  $\mu\text{g/mL}$  which is added after autoclaving the LB broth at 121°C for 20 min. The 5mL seed culture is incubated by shaking at 225 rpm overnight at 37°. This overnight seed culture is then added to 1L of LB and allowed to incubate by shaking at 225 rpm until the optical density (O.D) of the culture reaches ~0.55-0.75. IPTG is then added to the 1L culture to induce the cells and

overexpress the gene that encodes for GroEL. The induction process goes on for anywhere from 5 hours to 12 hours after which the stirring is discontinued. The IPTG is added later when the O.D is higher so that a certain minimum number of cells have been reached as the T7 RNA polymerase is extremely active which causes the cells to stop dividing due to the high energy requirements of the transcription and translation processes. The 1L cell culture is then spun by centrifugation in a Beckman Coulter Avanti JXN-30 centrifuge at 7000g's for 10 min. This separates out most of the cells from the cell culture solution by making the cells settle at the bottom of the centrifuge bottle. The spent LB is removed by pouring it out from the top. This concludes the expression protocol for wild-type GroEL which was used in the later experiments. The expression protocol used here proved to be very successful and efficient which will be proven in the following sections from the SDS page gels of the protein content of the cells and the proteins in the samples in every step of the purification process.

### 2.1.2 GroEL Purification

The purification of GroEL consists of 2 main parts. The first part includes the steps that separate the cell membrane and other major large components from the smaller components such as proteins. This will be discussed under the Lysis and Rudimentary Purification section. The next major part of purification is the separation of the desired protein from the other proteins. This will come under the section Advanced Purification.

The effectiveness of the purification which can be evaluated using analytical techniques will be discussed in the characterization section following purification.

#### 2.1.2.1. Lysis and Rudimentary Purification

The purification process for GroEL starts with the lysis of the cells. Lysis of the pelleted cells from the last step of the expression process involves freezing the cell pellet at -20 and then thawing it carefully. This is also referred to as the freeze-thaw method. A study conducted in the freeze-thawing of *E. coli* cells revealed that the freezing-related injuries to the cells were mainly due to the crystallization of the water surrounding the cells. In the case of the *E. coli* cells containing GroEL, the freezing of the water from the LB trapped between the cells in the cell pellet aids in lysis of the cells. The study also found that the addition of 10% glycerol substantially increased the cell survival rate which also points towards the crystallization of water being responsible for the lysis in the freeze-thaw method. This method is proven in this study to significantly weaken or break the cell membrane of *E. coli* cells.<sup>11</sup> Freeze-thawing of the cell pellet was then followed by resuspension of the thawed cell pellet in a lysis buffer containing 25 mM Tris-HCl (pH 7.5) and 1 mM Ethylenediaminetetraacetic acid (EDTA). Tris-HCl is the buffering agent of choice in this pH range and EDTA is a chelating agent that chelates metal ions thereby inhibiting the activity of proteases (which usually require metal ions as cofactors) which are also released into the solution with the lysis of the cells. The suspended form of the cells allows for easier further processing. The next step in the purification process is the sonication of the *E. coli* cells. This ensures the breakage of most of the cells, thus releasing

the protein and other contents of the cells. Sonication has been used to help in the lysis of *E. coli* as well as yeast and other bacterial strains. Sonication does not require sophisticated equipment or training and is generally very effective in lysing the cells thus making it an effective method for lysing bacterial cells to release intact recombinant protein from within the cells. The solution containing the intracellular proteins and the cell debris was then spun down at 20,000 g's to remove the broken cell membrane as well as other larger cell components. A 1-hour spin at 100,000 g's also helps get rid of any protein aggregates that might hinder the filtration process before the chromatography. The lysate is now ready for advanced purification processing.

#### 2.1.2.2. Advanced Purification

Advanced lysate purification consists of filtration of the supernatant that is obtained from after the centrifugation step in the previous step. The filtration is carried out using a 0.2 micron pore size filter that is attached to a luer lock syringe which contains the lysate. The lysate is then passed through the filter and collected to be heated. Since GroEL is a heat shock protein, which is a class of proteins that are produced as a response to heat stress experienced by the cell. They help in storage, protection or refolding of more heat-sensitive proteins which implies that these chaperone proteins are more resistant to the destructive effects of heat. This can be exploited in the purification process by heating the lysate with all the proteins in it at around 60°C which was found to be the optimum temperature that gives the greatest yield of GroEL while removing the maximum amount of other unwanted proteins through coagulation. Denaturation of proteins is one of the major causes for why

cells die when exposed to lethal heat. Proteins mediate a vast majority of the functions within a cell and are required for the survival of the cell. When exposed to heat, depending on the amount of heat, the quaternary structure of the protein is first disrupted, followed by the tertiary structure followed by the secondary structure and finally the primary backbone of the polypeptide chain that would become the protein when fully folded. This is in the order of increasing bond strength between the components of the protein in each level of structure. When the lysate is heated up to 60°C, majority of the proteins in the lysate denature on some level due to their thermal sensitivity as *E. coli* thrives at around 37°C. When proteins denature, more amino acids with charge on them hydrophobic sites are exposed to the solution. This leads to unlike charges and hydrophobic residues/sites attracting each other and forming clumps of material. These clumps of material are protein aggregates and eventually coagulate out of the solution. This coagulated material can be removed by simple centrifugation at around 20,000 g's for 20 minutes. The lysate is then passed through a vivaspin concentrator with a pore size of 100,000 kDa. This is a good enough pore size as GroEL has a size of 800,000 kDa and would not pass through the pores, thus getting concentrated. The clarified lysate at this point is ready for chromatography.

Two different types of chromatography techniques were used; Ion-Exchange Chromatography (IEC) and Size-Exclusion Chromatography (SEC). IEC uses the overall charge on the target protein to attract and adhere the protein to the resin in the IEC column. The overall charge on the protein is determined by the pH of the solution and the Ionization Point (pI). The theoretical pI of GroEL is around 4.85 as determined by an online

computational source using the gene sequence for GroEL. This means that if the pH of the surrounding buffer is greater than around 4.85, then the overall charge on GroEL will be negative and vice-versa. The magnitude of the overall charge on GroEL will depend on the magnitude of the difference between the pH of the buffer and pI of GroEL. Thus, for anion exchange, a pH of around 7.5 was selected for the buffer. This pH would give GroEL enough overall charge, allowing it to be removed using an anion exchange column. The ion-exchange step was used when the heat shock step was not employed to initially clarify the cell lysate. When the heat shock step is employed, most of the other proteins coagulate out of the solution, therefore not needing an IEC step before SEC. Since there are around 4,300 identified proteins in *E. coli*, a preliminary chromatography step such as IEC is usually employed before employing a more sensitive chromatography step such as the SEC so that the SEC column is not overwhelmed by the amount of proteins which leads to either no separation or an ineffective separation of the target protein. The proteins (both targeted and unwanted proteins) bound to the IE resin are eluted using an elution buffer and collected. The collected IE fractions with the target protein are then concentrated using a 100,000 kDa protein concentrator again to be injected into the SEC column. The SEC column is a chromatography column that separates proteins or other materials based on their size. The column is packed with porous resin containing pores of a certain size range. When the sample passes through the resin, the smaller proteins pass through the pores as they are small enough to fit through them while the bigger proteins can only fit through the inter-resin space. This means that the mean overall path of the smaller proteins is longer than that of the bigger proteins. Thus, the bigger proteins come out earlier and the smaller

proteins are delayed based on their size. The SEC fractions containing the target protein are then collected. The fractions collecting the target protein is identified from the chromatogram. The chromatograph contains a sensor for reading the absorbance of the collected fraction at 280 nm wavelength. The amino acids tryptophan and tyrosine have a specific absorbance peak at 280 nm which makes it easy to measure the amount of protein in any sample as long as there is negligible contamination from other components such as nucleic acids that might also absorb at 280 nm.<sup>12</sup>

### 2.1.3 GroEL Characterization

The amount of GroEL in a sample can be characterized using a variety of techniques that are commonly employed in protein research. The simplest of the techniques used here is the detection of protein using absorbance at 280 nm. Tryptophan and tyrosine both have a specific absorption peak at 280 nm wavelength due to the aromatic rings. Phenylalanine and disulfide bonds also have absorbance at this wavelength, but it is only significant when tryptophan and tyrosine are absent and there are enough protein molecules containing enough phenylalanine and disulfide bonds.<sup>12</sup> A more reliable way to characterize the amount of GroEL is by using Sodium Dodecyl Sulphate - Polyacrylamide Gel Electrophoresis (SDS-PAGE) gels. The third and the last way of characterization of GroEL carried out in the following experiments is using Electron Microscopy (EM) imaging.

#### 2.1.4 Assembly and Characterization of Platinum Nanoparticles

Platinum nanoparticles were made using GroEL as the capping agent. To synthesize platinum nanoparticles, GroEL is added to the required amount of water and  $\text{K}_2\text{PtCl}_4$ , where GroEL is at  $5\mu\text{M}$  final concentration and  $\text{K}_2\text{PtCl}_4$  is at  $3\text{mM}$  final concentration. The last ingredient is the reducing agent which is  $\text{NaBH}_4$  which is at  $15\text{mM}$  final concentration. The water used here is the volume that would bring the total volume to that which was used in the calculation of the other ingredients. This mixture, when left over 16-24 hours develops a brownish color which is indicative of the nanoparticles. The nanoparticles produced are characterized using TEM and cryoEM in these studies.

#### 2.1.5 Crystallization of GroEL

Crystallization of GroEL was carried out using the sitting-drop method. This involves placing the GroEL crystallization droplet on a pedestal which is surrounded by the crystallization reagent. The wells are then sealed air-tight so that the diffusion process can occur. Three main crystallization conditions were discovered in the crystallization studies conducted are mentioned in the pictures of the crystals below. The crystallization process occurred at room temperature and pressure which were approximately  $21^\circ\text{C}$  and 1 atm. The crystal formation was observed under a Leica MC170 HD 1x – 12x microscope.

## 2.2. Results and Discussion

The purification process of GroEL using the heat-induced-coagulation method proved very effective in separating GroEL from other proteins with high efficiency and purity. This can be visualized from the following SDS-PAGE gels which show the samples from successive steps in the purification process.

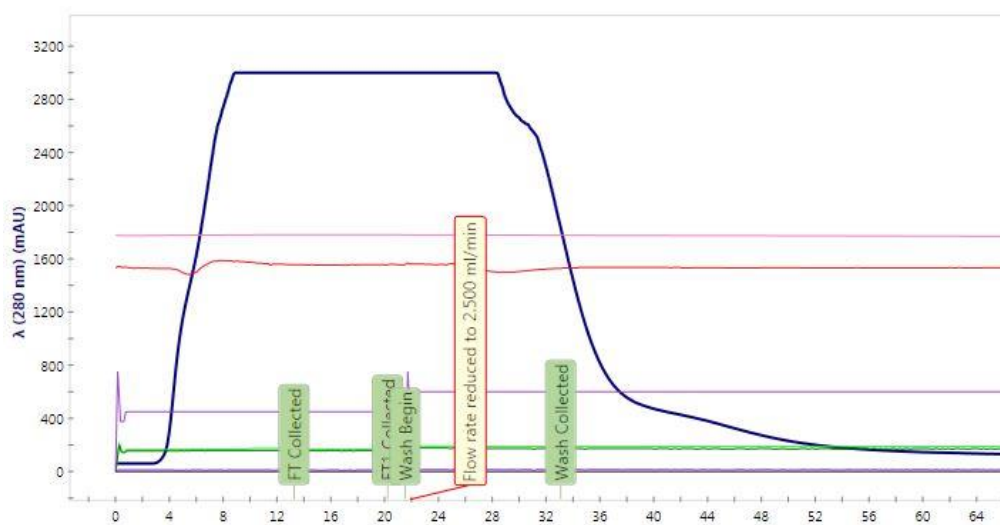


Figure 1: Load and wash steps of IE chromatogram of GroEL where the lack line shows the % of elution buffer, blue line shows the absorbance at 280 nm which indicates protein presence and the red line shows the conductivity

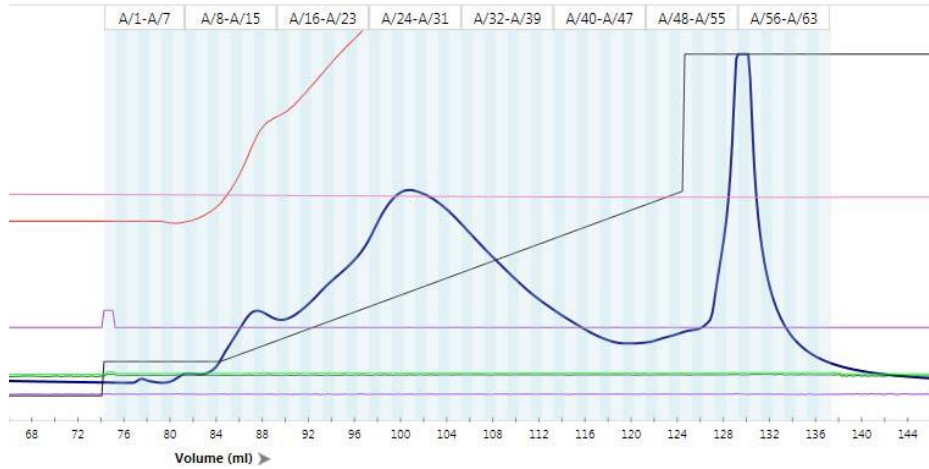


Figure 2: The elution part of the IE chromatogram for GroEL

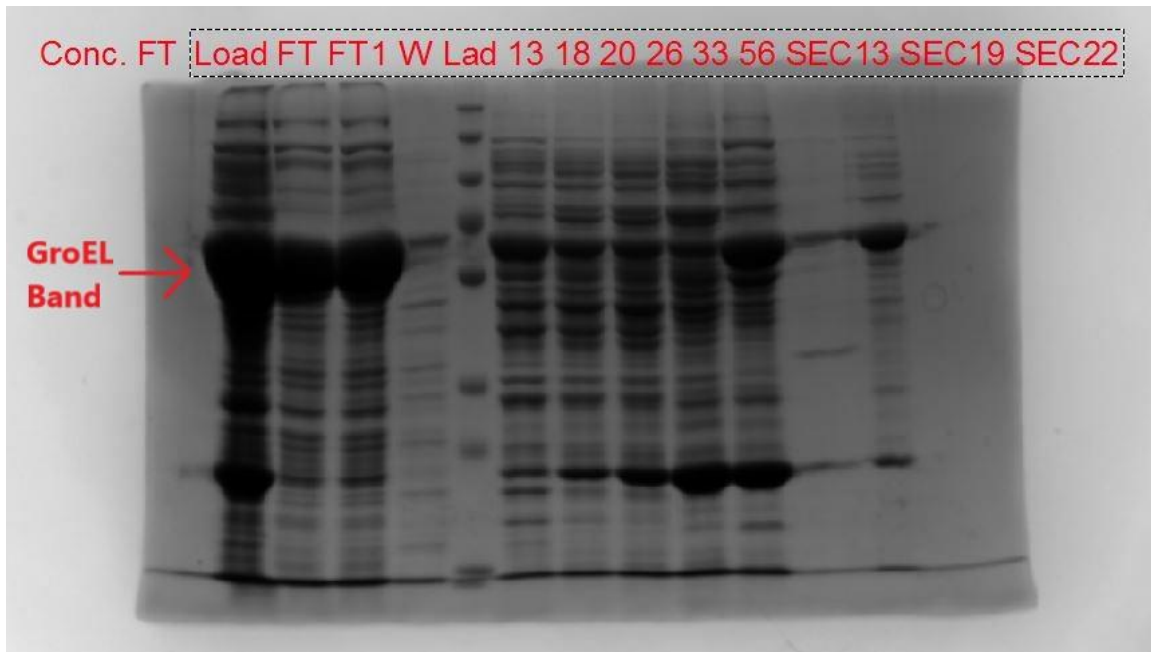


Figure 3: SDS-PAGE gel of the IEC step in GroEL purification shown from the above chromatogram pictures along with the collected SEC fractions after the IEC, where FT refers to Flow Through, W refers to Wash

The above chromatogram and the SDS-PAGE gel corresponding to the chromatogram shows that the process does obtain a pure enough GroEL sample, but it is very inefficient

as a significant amount of the GroEL is being lost in the flow through and wash steps of ion exchange chromatography. This results in a very low concentration as well as insufficient purity after one IEC followed by one SEC step. To help increase the yield and purity, the heat resistance of GroEL was exploited for a better purification process. The results of the SEC performed after heat shock of the GroEL lysate is seen below.

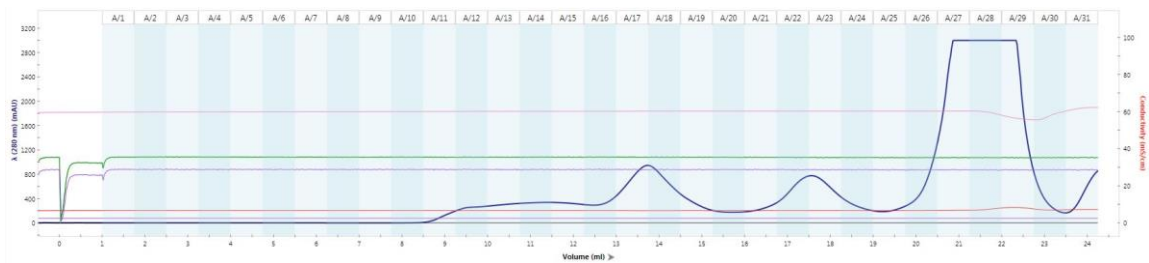


Figure 4: Chromatogram of the SEC step performed after heat purification step applied to GroEL lysate



Figure 5: SDS-PAGE gel of the above SEC step for GroEL purification using heat shock method

From the heat shock SDS-PAGE gels, it is evident that the band of the GroEL obtained after SEC purification is significantly clearer of other contamination. This can be visualized from the difference in the thickness of the other bands relative to the thickness of the GroEL band. Apart from containing a small amount of contaminating material, the collected SEC fractions also had a large amount of GroEL, a large percent of which was fully folded in the quaternary structure as can be seen from the cryoEM data that was collected which is presented further in this work. The higher concentration of GroEL allowed for multiple experiments from this sample and was concentrated enough to conduct crystallization experiments.

The purified GroEL was used to produce protein crystals in the sitting-drop configuration as can be seen from the pictures below.



Figure 6: A photograph of GroEL crystals formed when GroEL concentration was at 40mg/mL (1:1 on pedestal) and reservoir solution consisted of 0.1M Sodium Citrate at pH 5.3, 11% PEG 6000

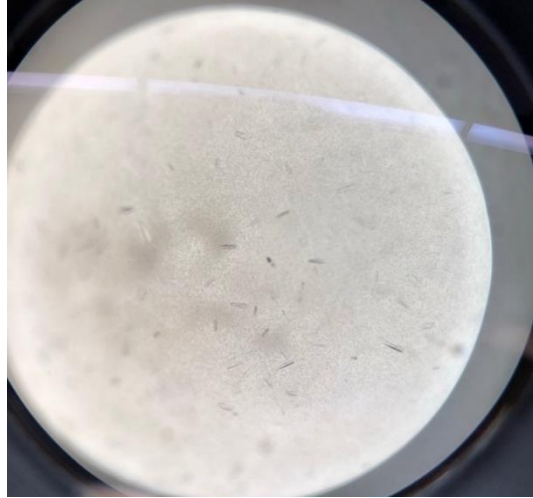


Figure 8: A photograph of GroEL crystals that formed when GroEL concentration was 54 mg/mL (1:1 – protein:reagent on pedestal) and reservoir solution consisted of 0.3% PEG 8000, 1.72M ammonium sulfate, 0.004M calcium chloride and 0.1M Tris-HCl at pH 8.0

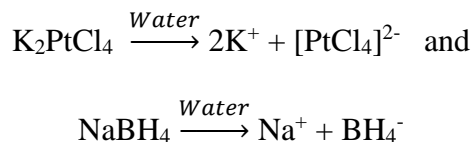


Figure 7: A photograph of GroEL crystals that formed when GroEL concentration was at 40mg/mL (1:1 on pedestal) and reservoir solution consisted of 0.1M Sodium Citrate at pH 5.4, 9% PEG 6000

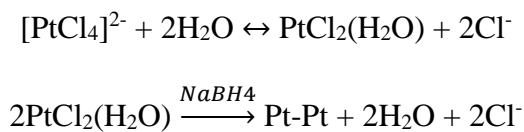
The above crystals were set to be incubated in platinum nanoparticles with the reducing agent before cryo-freezing so that the formed nanoparticles would adhere to the site of formation on the GroEL surface or insides which can then be analyzed through x-

ray crystallography. This was not possible due to the small size of the crystals and the large size of the Groel, both of which worked against getting good diffraction data.

The purified GroEL when mixed with platinum ions and the reducing agent NaBH<sub>4</sub> produced a nanoparticle solution which is indicated by the brownish color that developed overnight. This when compared with controls that contain only the platinum ions with a reducing agent shows that in the absence of protein to cap the metal platinum formation, black deposition of metal platinum around the walls of the Eppendorf tube in which the reaction was carried out. This is because in the absence of a capping agent to control the size of the metallic platinum formed, bulk platinum is formed from the platinum ions reduced from the solution by NaBH<sub>4</sub>. Initially in the presence of water, K<sub>2</sub>PtCl<sub>4</sub> and NaBH<sub>4</sub> dissociate and ionize as:



Then the reduction of Pt proceeds as:



In the presence of only platinum ions and GroEL without the reducing agent, it was observed from long time storage that the GroEL would form aggregates. When stored over extended periods of time, the solution turns cloudy indicating bulk macroscale protein

aggregation. This claim is further reinforced through a change in pH over 24 hours as well as cryoEM screening.



Figure 9: Eppendorf tubes holding metallic platinum reduced from ions by  $\text{NaBH}_4$  in the absence of protein (left) and platinum nanoparticles in the presence of GroEL (right)



Figure 10: GroEL in the presence of platinum ions ( $\text{K}_2\text{PtCl}_4$ ): Left – Immediately after addition, Right – After storage for a month



Figure 11: Eppendorf tubes showing the comparison of platinum nanoparticle formation using GroEL (two tubes on the left) versus bulk platinum formation in the absence of GroEL



Figure 12: Low contrast photograph of platinum nanoparticles versus bulk platinum

CryoEM screening reveals the affinity of the protein aggregates to the sides of the grid which reveals the hydrophobic nature of the protein aggregates. GroEL being an ~800kDa protein clearly shows the 4 ring structures in the side view and a circular footprint from the top or bottom view when the protein is fully folded in its quaternary structure. The absence of these clearly defined structures in the samples with only GroEL and

platinum ions reveals the breakdown of the quaternary, tertiary as well as secondary structures in some areas of the grid.

The nanoparticle formation was further investigated using the negative staining method using TEM and cryoEM. Upon further image processing and 3D model construction, it was conclusive that nanoparticles were forming in the inner cavity of GroEL which is shown by the abnormally high density in two areas.

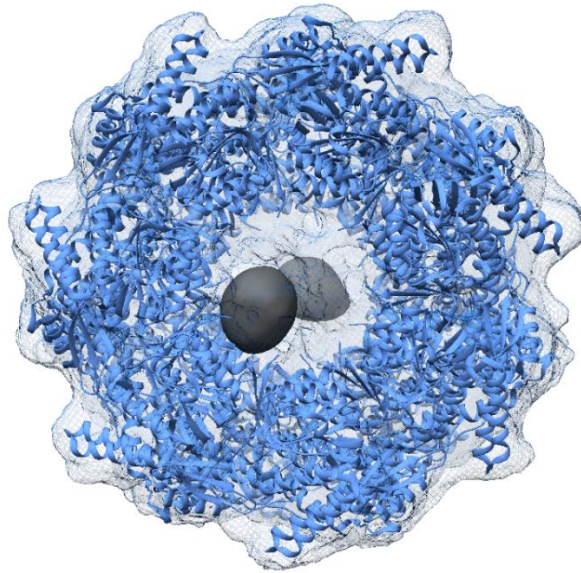


Figure 13: 3D reconstruction of GroEL (top view) showing two regions of higher density in the center cavity

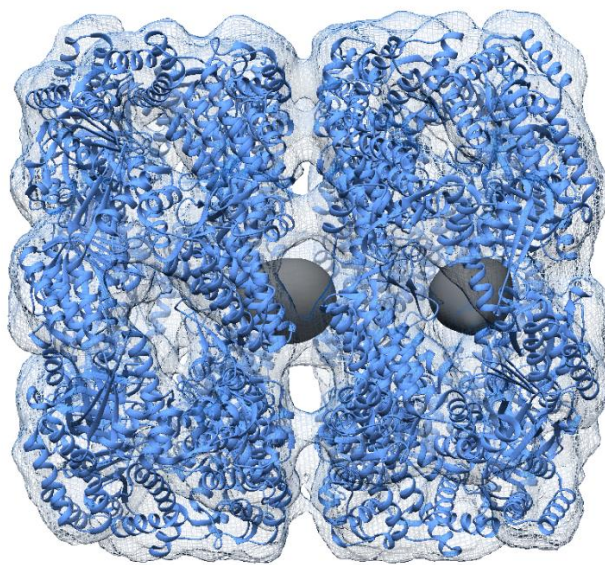


Figure 14: Side view of 3D reconstruction of GroEL showing the higher density regions in the center when superimposed with the 3D structure of only GroEL

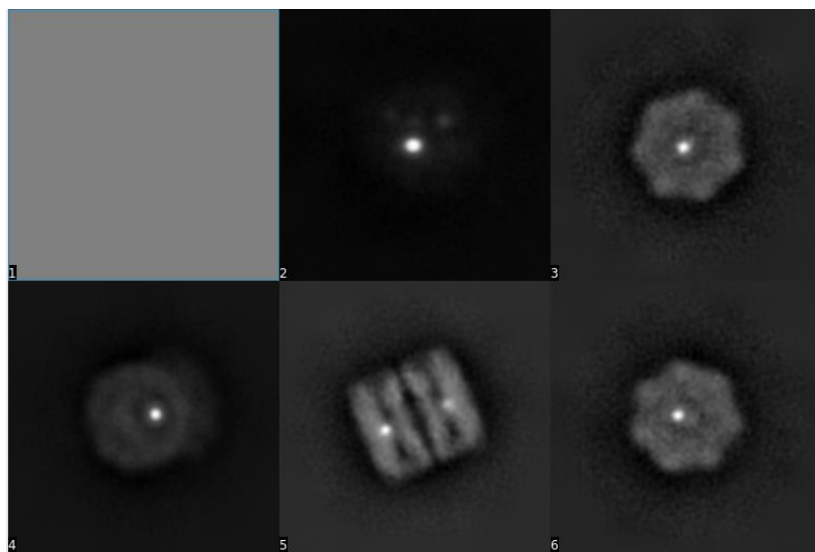


Figure 15: CryoEM pictures after data refining showing a distinct region of hypothesized nanoparticle formation inside the GroEL cavity

The refined data indicates strongly that the platinum nanoparticles are being formed on the inside of the GroEL. But this does not rule out the possibility of platinum nanoparticles forming elsewhere. Further analysis using cryoEM could reveal the exact method by which GroEL helps form nanoparticles along with possible sites on GroEL surface that provide favorable conditions that aids in the formation of platinum nanoparticles

## Chapter 3

### INTERACTION OF MBP WITH GOLD

Maltose Binding Protein (MBP) is a 396 amino acid long protein with a mass of around 43.4 kDa.<sup>13</sup> It has been extensively used as a fusion protein to purify proteins that were hard to purify. It was small enough to be attached to a lot of larger proteins and then the target protein-MBP complex could be purified using an affinity column before the MBP is cleaved off and removed, leaving the purified target protein behind. MBP was found to produce gold nanoparticle in the presence of gold ions and HEPES, which is a mild reducing agent. Further analysis using UV-vis spectrophotometry, Dynamic Light Scattering (DLS), mass spectrometry and color change observation was conducted to characterize the synthesized gold nanoparticles. Analysis using electron diffraction revealed that gold ions had a specific affinity to one site on the MBP protein where the gold nanoparticles seemed to be forming. A peptide with the same amino acid sequence as that of the site of formation of gold nanoparticles on the MBP protein was used to test the effect of the major amino acids in that location. After studies on it, it was concluded that the new peptide is also capable of producing gold nanoparticles. Studies on a few other peptides very similar to the peptide tested above also had some interesting results which will be discussed in detail below.

## 3.1 Experimental Materials and Methods

### 3.1.1 MBP Expression and Purification

MBP was expressed in a pET vector in an *E. coli* cell culture. A 1 L culture of *E. coli* was expressed and purified using most of the techniques used in GroEl purification with the exception of some steps. MBP is not a very thermostable protein and thus the heat treatment was not employed for MBP. MBP also has a specialized dextrin-based chromatography column which removes MBP specifically from the lysate through affinity chromatography. MBP binds to dextrin through hydrogen binding and it is highly specific so only MBP gets separated from the lysate and it is usually almost 100% pure. This almost eliminates the need for an SEC step after affinity chromatography, but the SEC step is performed to remove any protein aggregates or contamination from any unexpected sources. After the SEC step, the MBP sample is ready to be used for the gold nanoparticle experiments.

### 3.1.2 Gold Nanoparticle Experiments

All the gold nanoparticle experiments were carried out using MBP and 5 of the peptides derived from MBP. The protein/peptide was used as a capping agent and when mixed with gold ions and HEPES, gave some interesting results. The peptide/protein was added first to the 96 plate UV-vis plates, followed by water, followed by gold ions and then finally HEPES right before the UV-vis readings were taken. This is because the reaction to

produce metallic gold nanoparticles begins immediately after the addition of HEPES. The major peptide used in this study is the peptide named 'AT1' whose sequence is 'YPPGGSGGSGM'. The other peptides were made from AT1 by replacing one major reactive amino acid (tyrosine, proline, methionine and phenylalanine) in each peptide with an unreactive alanine. The final peptide which is the control is alternated sequence of serine and glycine. The serine and glycine amino acids in the peptide chains confer flexibility to the amino acid backbone whereas replacement of the major amino acids with alanine is to eliminate the side chain after the  $\beta$ -carbon, does not change the main chain conformation significantly and does not display extreme steric or electrostatic effects.<sup>16</sup>

### 3.2 Results and Discussion

The addition of HEPES to gold ions in solution in the presence of MBP or the appropriate peptide can be seen to form nanoparticles due to its characteristic red color which is significantly different from the gold/yellow color of metallic gold. The confirmation for nanoparticle formation as well as the quantification of the kinetics of nanoparticle formation over time can be done through UV-vis spectroscopy. A wavelength scan at 18 hours into the experiment from 400 nm to 750 nm shows the presence of spherical gold nanoparticles which is indicated by the peak absorbance at around 530 nm.<sup>17</sup> This can be seen in the data collected below. This also reveals the stability of the synthesized gold nanoparticles over time. The sample with the control peptide, as seen below, does not show a distinct peak at around 530 nm which was accompanied by a visible change in the tint of

red for the control. This indicates that the control peptide, as expected, does not synthesize nanoparticles. The increased base absorption across all the wavelengths for the control is most likely due to bulk gold formation through reduction by HEPES. One interesting observation from this plot is that the graph for the sample with the peptide with the tyrosine replaced by alanine resembles that of the control peptide.

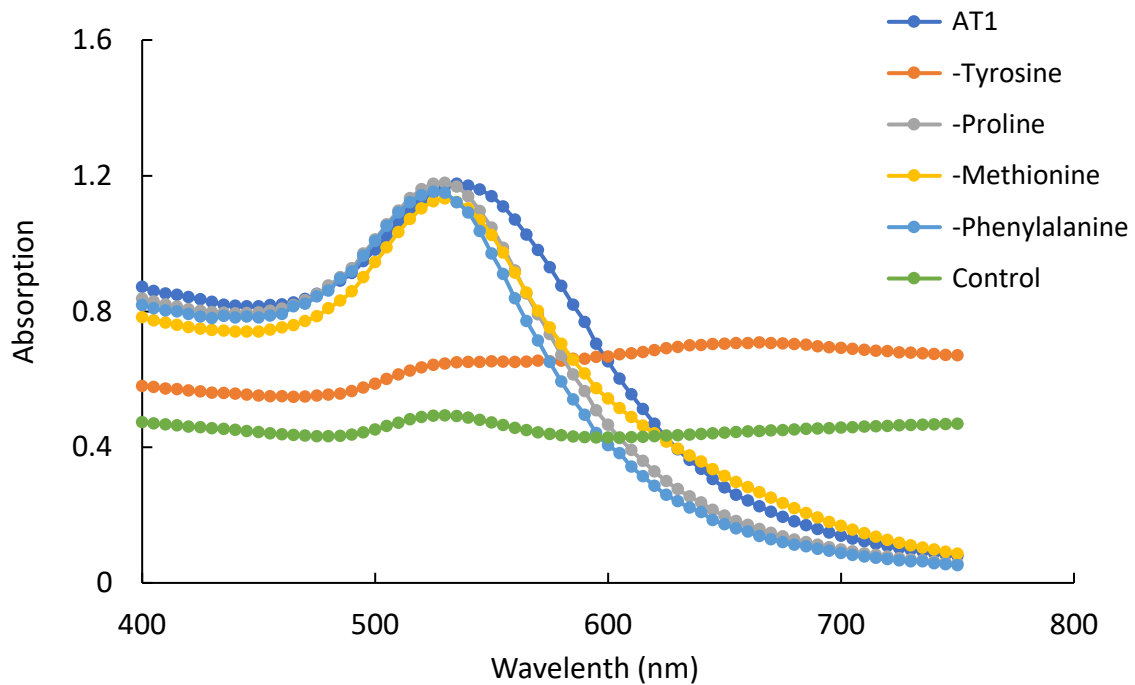


Figure 16: Data of the wavelength scan at t=18 hours of different peptides including a control peptide.

This data collected implies that tyrosine is important for the synthesis of gold nanoparticles. One observation that can be made is that out of the 4 major peptides in AT1, 3 of them contain cyclic structures with the only exception being methionine. The ring structures are

expected to interact with gold ions which creates favorable environments for the formation of gold nanoparticles.

## Chapter 4

### Car9 TAG STUDIES

#### 4.1 Introduction to Car9 Tag

Car9 is a silica-binding affinity tag that was developed by a lab in the University of Washington. It was developed with the goal of creating a peptide tag that can be attached to the C-terminal end of a protein to be used for fast and effective purification of the protein. The tag was previously observed to have an ability to bind specifically to carbonaceous substrates and silica (through electrostatic and  $\pi - \pi$  interactions), both of which are abundantly available on earth. This would greatly reduce the cost and time of purification of proteins that are hard to purify using traditional low-cost methods and ideally replace the use of hexahistidine (His) tags in protein purification.<sup>14</sup> Further studies were carried out on incorporating the Car9 tag into one of the native amino acid loops of the protein that extend out considerably from the surface of the protein. This is to allow the study of adhesion of the Car9 tag to carbonaceous substrates through x-ray crystallography. When the Car9 tag is present at the C-terminal of a protein, it is allowed to flex, which is thought to be important for the conformation of the tag which endows the tag its carbonaceous substrate/silica-binding ability. But this flexing of the tag is not desirable for x-ray crystallography as the tag would have a different special conformation in each unit cell,

thus giving bad data in the region of the Car9 tag. The following studies were conducted on Car9 modifications on sfGFP and  $\beta$ -galactosidase.

#### 4.2 Materials and Methods

Mutated versions of sfGFP, GroEL and  $\beta$ -galactosidase were created using the Car9 tag in loops that extend out from the proteins. Simple gravity columns were used to hold the silica resin while the lysate was made to flow through the packed silica resin bed. This method ensured maximum contact and represented the purification results for a more realistic and applicable purification strategy for Car9 tagged proteins. The silica resin used in this application was of pore size 60Å, 70-230 mesh and 63-200 $\mu$ m in size. The cell culturing, pelleting, freezing and lysis were all performed for sfGFP, GroEL and  $\beta$ -galactosidase as was performed for MBP and GroEL. After lysis, instead of an IEC step, it was dialyzed against a wash buffer which consisted of 25mM Tris-HCl and 2mM EDTA after which it was passed through the gravity column, followed by a wash step with only the wash buffer, followed by an elution step in which the elution buffer contained the same ingredients as that of the wash buffer along with 1M L-lysine. The elution fractions were collected and analyzed for the presence of the target protein using SDS-PAGE gels and the fractions that included the target proteins could then be passed through an appropriate SEC column which removes most of the other contaminants or protein aggregates. A quick method to test the presence of  $\beta$ -galactosidase is from a colorimetric assay using the compound O-Nitrophenyl- $\beta$ -D-galactopyranoside (ONPG). ONPG can be used as the substrate for  $\beta$ -

galactosidase which cleaves the ONPG into  $\beta$ -D-galactose and O-nitrophenol. O-nitrophenol is a yellow colored compound and thus the presence of active/functional  $\beta$ -galactosidase can be verified by adding a small volume of the sample to ONPG and the development of a distinct yellow color is indicative of the presence of  $\beta$ -galactosidase.

### 4.3 Results and Discussion

After extensive analysis of different Car9 loop systems in different proteins, it was concluded that the Car9 tag was not functional as a loop in this state. The following data provides some insight into how it was concluded that the loop is not functional.

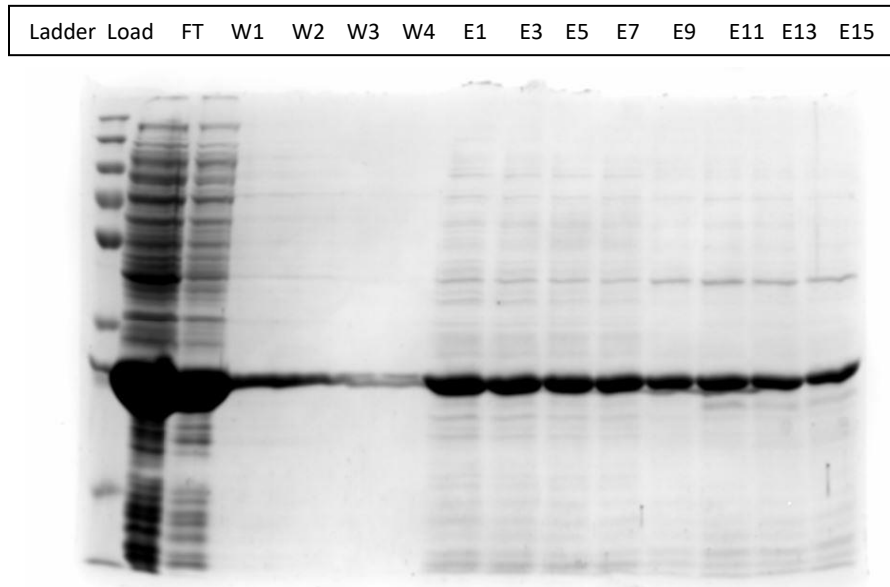


Figure 17: SDS-PAGE gel showing elution fractions of sfGFP::Car9 -5aa flowing through a silica bed in a gravity column after being incubated in the silica resin for 16 hours at 4°C

Ladder	Load	FT	W1	W2	W3	W4	E1	E3	E5	E7	E9	E11	E13	E15
--------	------	----	----	----	----	----	----	----	----	----	----	-----	-----	-----

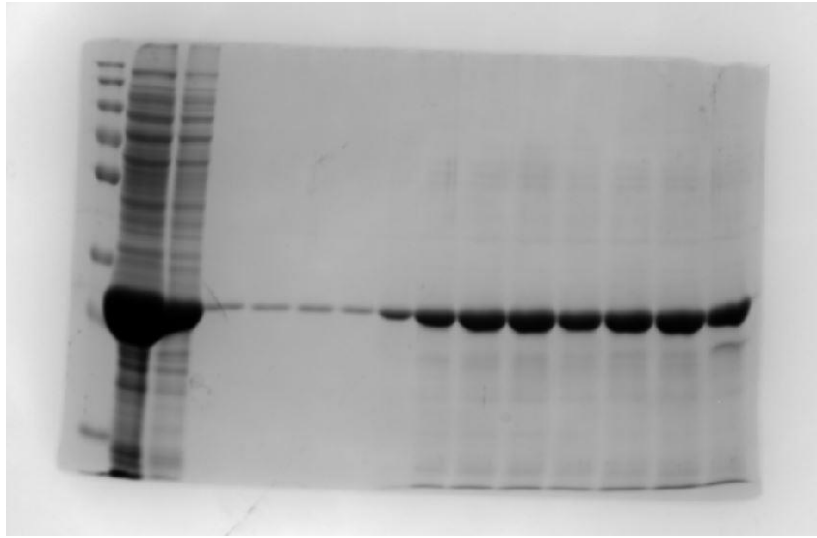


Figure 18: SDS PAGE gel showing the elution volumes for sfGFP::Car9 when flowing the lysate through the silica bed in a gravity column after incubation for 16 hours at 4°C

From the above 2 graphs, the binding of sfGFP::Car9 and sfGFP::Car9 -5aa to silica resin of 60Å can be quantified. Upon analysis of the gels, it can be said that the binding of both the Car9 variants of sfGFP used here do not have any specific binding to silica. The binding is very unspecific as it can be seen that the other bands present in the lysate are visible as well. The reduction of the band intensities of all the bands on the gel are almost comparable in the elution fractions. This indicates that the binding is non-specific, and the elution buffer is helping bring all the bound proteins. If the sfGFP::Car9 was binding to silica specifically due to the Car9 tag, the elution fractions should either be a much stronger band

for sfGFP compared to the other bands or the other protein bands should be essentially invisible.

GroEL showed a very similar pattern when the lysate was flowed through a gravity column containing 500 Å pore size silica resin.

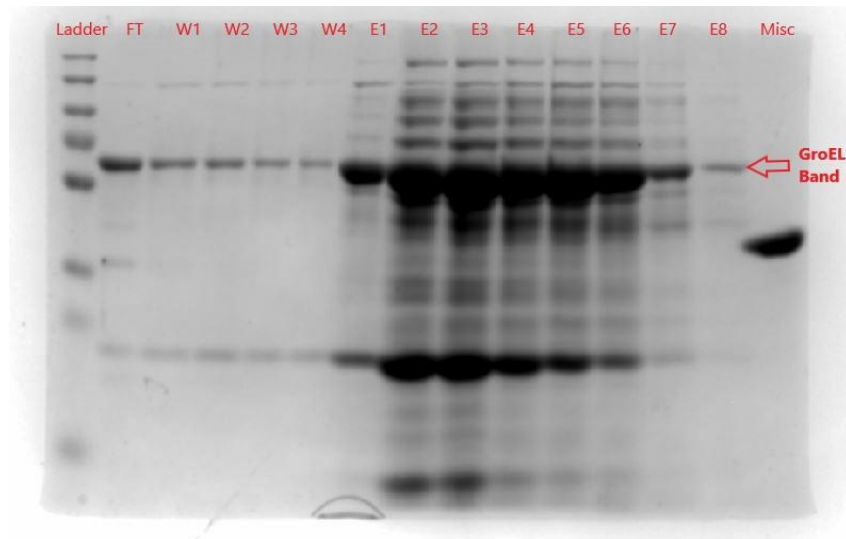


Figure 19: A photograph of the SDS-PAGE gel of the fractions collected by flowing wildtype GroEL through a silica resin bed and eluted using 1M L-lysine

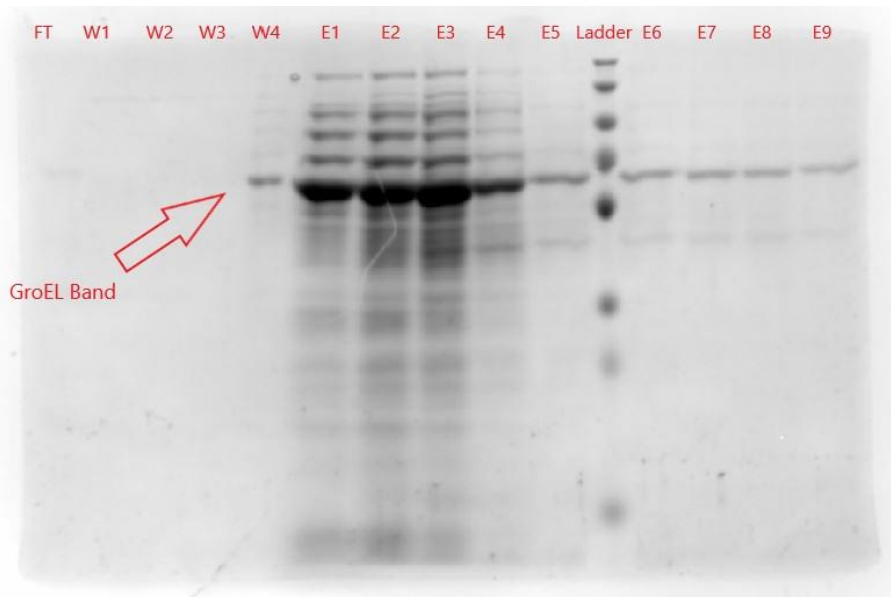


Figure 20: A photograph of the SDS-PAGE gel analysis of the fractions collected when GroEL containing the Car9 tag in a loop was flowed through silica resin and eluted with 1M L-lysine

Both the above photographs of the SDS-PAGE gels of the wildtype GroEL versus the Car9 loop groEL were from experiments performed under the same conditions and the same elution volumes were collected to be able to compare with one another. From comparison, it can be seen that the wildtype GroEL sticks to the silica with the same specificity as that of the Car9 loop GroEL, thus showing that the Car9 loop in this mutation of GroEL does not confer any special affinity towards carbonaceous or silica-based substrates. This further adds to the conclusion provided by the sfGFP that when the Car9 tag is being added to proteins in a native loop, it does not display its ability to attach onto carbonaceous substrates. This could be due to a multitude of reasons, but the one reason that is most probable is that the structural conformation that the Car9 tag can achieve while being attached to the C-terminal end of the protein is not reproduced when it is in the form of a

loop. This is thought to stop the Car9 tag from achieving proper placement of charges as well as the important residues which would eventually allow for adhesion to carbonaceous substrates.

The Car9 loop when attached to  $\beta$ -galactosidase was analyzed using the same method as sfGFP and GroEL. It was passed through a gravity column containing a silica resin bed. The load was compared to the elution fractions using the colorimetric ONPG assay which revealed that while the load contained a significantly large amount of  $\beta$ -galactosidase, the elution volumes had none. This indicates that all the functional  $\beta$ -galactosidase had been removed from the column in the wash step along with all the other proteins in the lysate meaning that the Car9 tag did not function as was expected.

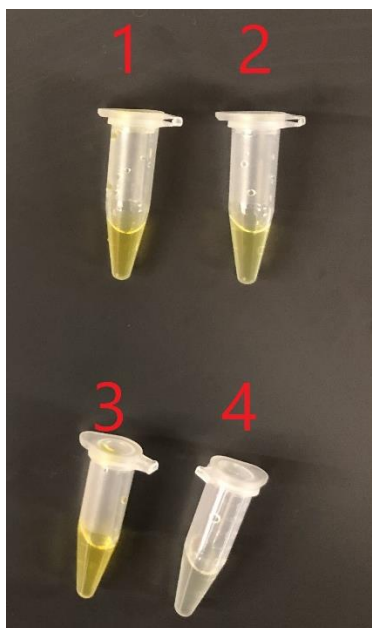


Figure 21: ONPG test results of the  $\beta$ -galactosidase samples in the Car9 testing: 1 - Load, 2 - Flow through, 3 - Wash, 4 - Elution using 1M L-lysine

From the results of the ONPG test as seen from above, it is evident that  $\beta$ -galactosidase is abundant in the sample that is loaded onto the silica resin column, flow through coming out of the column and wash flow and also that there is barely any or no functional  $\beta$ -galactosidase in the elution flow from the column.

Another test performed on a smaller scale involved incubating the lysate containing  $\beta$ -galactosidase with a small amount of silica resin in an Eppendorf tube. The incubation, which was done by slow inversions of the tube, would ensure that the Car9- $\beta$ -galactosidase in the lysate would have enough time to adhere to the silica resin. After an hour of

incubation at room temperature, the resin was allowed to settle and ONPG was introduced into the Eppendorf tube and lightly agitated initially to evenly distribute ONPG.



Figure 22: Eppendorf tube after incubation with ONPG showing the silica resin region displaying very little to no yellow color but the supernatant showing a bright yellow color

The silica resin region of the tube not turning yellow shows that either the Car9- $\beta$  galactosidase attached to the silica is not functional or that little to none of the Car9- $\beta$  galactosidase adhered to the resin. Both these results are not desirable because if the Car9 loop makes the  $\beta$ -galactosidase non-functional, it would have to be moved to another native loop on  $\beta$ -galactosidase.

### CONCLUSIONS AND FUTURE WORK

#### 5.1 Inorganic Nanoparticle Synthesis Using Proteins and Peptides

With the MBP-Gold experiment results and the GroEL-Platinum studies conducted, it becomes evident that proteins and peptides can be used to potentially mass manufacture nanoparticles. But there is no denying the fact that more studies and understanding of the process is required in order to achieve more control over the nanoparticle synthesis. Further understanding of the GroEL-platinum interaction could be achieved through a time-resolved cryoEM analysis of the platinum nanoparticle formation. This would also give further insight into the kinetics of the nanoparticle formation. One major goal would be the identification of specific sites on GroEL that facilitate formation of platinum nanoparticles. This would allow the creation of specialized peptides that resemble the original site on GroEL which could be used to produce platinum nanoparticles without the need for the entire GroEL structure, thus making the nanoparticle synthesis process more efficient and potentially easy to control. For the MBP-Gold studies, new peptides should be made that contain only tyrosine at the end without any of the other major amino acids which are not serine and glycine. The other major amino acids can be substituted by alanine which holds the structural integrity of the peptide while not reacting with gold or any other compound in its environment.

## 5.2 Car9 Tag

The Car9 tag is proven to be quite effective when present in the C-terminal end of a protein when present in smaller proteins such as sfGFP. This is yet to be explored with other larger and complex proteins such as  $\beta$ -galactosidase and GroEL. There is good reason to believe that this has potential to be very useful in purifying proteins that are hard to purify by themselves and in situations where fusion proteins or other methods would not be effective methods to purify the protein from a lysate. One example of potential application is in the purification of membrane proteins. Since the tag is small and could potentially be integrated into one of the native amino acid loops in the protein, it might not disrupt the function or structure of the protein while allowing the protein to have hydrophobic/hydrophilic domains without any changes so that it will not be destroyed due to conformational changes. Car9 tag as a loop within the protein's amino acid backbone is yet to be explored properly and proven for use in other proteins. The Car9 tag is still in its initial stages of development and it could have a significant impact on protein purification on a world scale if successful.

## REFERENCES

1. Skinner, H. C. W., & Jahren, A. H. (n.d.). Biomineralization. In *Treatise on Geochemistry*(Vol. 8, pp. 1–69). Elsevier.
2. Dodd, M. S., Papineau, D., Grenne, T., Slack, J. F., Rittner, M., Pirajno, F., ... Little, C. T. S. (2017). Evidence for early life in Earth's oldest hydrothermal vent precipitates. *Nature*, *543*(7643), 60–64. doi: 10.1038/nature21377
3. Lengke, M. F., Fleet, M. E., & Southam, G. (2006). Morphology of Gold Nanoparticles Synthesized by Filamentous Cyanobacteria from Gold(I)–Thiosulfate and Gold(III)–Chloride Complexes. *Langmuir*, *22*(6), 2780–2787. doi: 10.1021/la052652c
4. Hainfeld, J. F., Slatkin, D. N., & Smilowitz, H. M. (2004). The use of gold nanoparticles to enhance radiotherapy in mice. *Physics in Medicine and Biology*, *49*(18). doi: 10.1088/0031-9155/49/18/n03
5. Pissuwan, D., Valenzuela, S. M., & Cortie, M. B. (2006). Therapeutic possibilities of plasmonically heated gold nanoparticles. *Trends in Biotechnology*, *24*(2), 62–67. doi: 10.1016/j.tibtech.2005.12.004
6. Khan, I., Saeed, K., & Khan, I. (2017). Nanoparticles: Properties, applications and toxicities. *Arabian Journal of Chemistry*. doi: 10.1016/j.arabjc.2017.05.011
7. Bensebaa, F. (2013). Optoelectronics. *Interface Science and Technology Nanoparticle Technologies - From Lab to Market*, *19*, 429–479. doi: 10.1016/b978-0-12-369550-5.00007-0
8. Braig, K., Otwinowski, Z., Hegde, R., Boisvert, D. C., Joachimiak, A., Horwich, A. L., & Sigler, P. B. (1994). The crystal structure of the bacterial chaperonin GroEL at 2.8 Å. *Nature*, *371*(6498), 578–586. doi: 10.1038/371578a0
9. pET System Manual. (n.d.). *pET System Manual*.
10. (n.d.). LB Broth and LB Agar. Retrieved from <https://www.thermofisher.com/us/en/home/life-science/cell-culture/microbiological-culture/bacterial-growth-media/lb-broth-and-lb-agar.html/>

11. Souza, H. (1980). Studies on the damage to Escherichia coli cell membrane caused by different rates of freeze-thawing. *Biochimica Et Biophysica Acta (BBA) - Biomembranes*, 603(1), 13–26. doi: 10.1016/0005-2736(80)90387-9
12. Man, T. P. (2016, February 17). Why Does Tyrosine and Tryptophan Have Effect in Protein Determination and to What Degree? Retrieved from <https://info.gbiosciences.com/blog/why-does-tyrosine-and-tryptophan-have-effect-in-protein-determination-and-to-what-degree>
13. UniProt ConsortiumEuropean Bioinformatics InstituteProtein Information ResourceSIB Swiss Institute of Bioinformatics. (2019, July 31). Maltose/maltodextrin-binding periplasmic protein. Retrieved from <https://www.uniprot.org/uniprot/P0AEX9>
14. Coyle, B. L., & Baneyx, F. (2014). A cleavable silica-binding affinity tag for rapid and inexpensive protein purification. *Biotechnology and Bioengineering*, 111(10), 2019–2026. doi: 10.1002/bit.25257
15. Sennuga, A., Marwijk, J. V., Boshoff, A., & Whiteley, C. G. (2012). Enhanced activity of chaperonin GroEL in the presence of platinum nanoparticles. *Journal of Nanoparticle Research*, 14(5). doi: 10.1007/s11051-012-0824-6
16. Lefevre, F. (1997). Alanine-stretch scanning mutagenesis: a simple and efficient method to probe protein structure and function. *Nucleic Acids Research*, 25(2), 447–448. doi: 10.1093/nar/25.2.447
17. Jain, P. K., Lee, K. S., El-Sayed, I. H., & El-Sayed, M. A. (2006). Calculated Absorption and Scattering Properties of Gold Nanoparticles of Different Size, Shape, and Composition: Applications in Biological Imaging and Biomedicine. *The Journal of Physical Chemistry B*, 110(14), 7238–7248. doi: 10.1021/jp057170o